THE JOURNAL OF PHYSICAL CHEMISTRY B

Article

pubs.acs.org/JPCB

Growth of Isotropic Domains As a Mechanism of Dynamic Diffraction Grating Recording in Low Molecular Liquid-Crystalline Derivatives of Azobenzene

Maciej Czajkowski,* Stanislaw Bartkiewicz, and Jaroslaw Mysliwiec

Wroclaw University of Technology, Wybrzeze Wyspianskiego 27, 50-370 Wroclaw, Poland

ABSTRACT: In this paper, we propose and explain the mechanism of dynamic molecular motions and isotropic domain formation during the diffraction grating recording in low molecular liquid-crystalline azobenzene derivatives. The photochromic molecules of 4-heptyl-4′-methoxyazobenzene, showing nematic liquid-crystalline properties close to the room temperature (from $T = 34$ °C), are used. A one-dimensional model of the grating formation is formulated based on in vivo polarized microscope observations. Formation and growth of the isotropic domains induced by the sinusoidally modulated Gaussian light intensity distribution is proposed as the mechanism and is used for experimental data fitting. The influence of the recording light intensity, grating period, and temperature on the domain growth rate factor is checked.

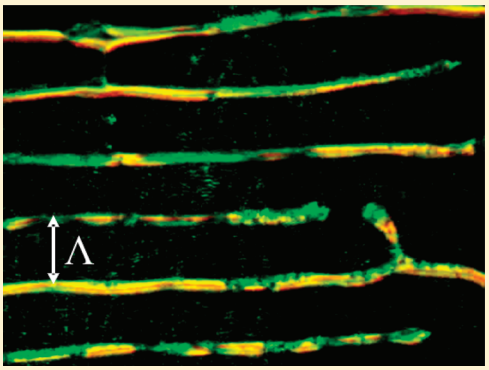

1. INTRODUCTION

Photochromic liquid crystals are a group of materials in which light can induce a transition from the liquid-crystalline to isotropic phase.[1] Moreover, in mixtures of photochromic molecules and liquid crystals, the light-induced phase separation process can occur.[2,3] Both light-induced processes are accompanied by the change of refractive index of the material. The control of this property at the micro- or nanoscale gives the materials potential for use in all-optical devices. The response of liquid crystals doped with azobenzene derivatives on absorbed light was studied earlier in pump−probe[1,2,4,5] and holographic setups.[6,7]

Photoinduced phase transition in liquid crystals doped with azobenzene derivatives was studied earlier under the polarized microscope.[8,9] A uniform UV light of wavelength $\lambda \approx 365$ nm was used for photoinduction of the *nematic-to-isotropic* (N → I) phase transition. Sung et al.[8] have assumed that the isotropic phase appears as a microscopic domain, formed around the cis isomer of azobenzene derivative molecules. Their model is based on randomly positioned formation and growth of circularly shaped isotropic domains, characterized by the constant growth rate of their radius during the irradiation.

In our previous article, we reported the results of transient diffraction grating recording in one-component liquid-crystalline azobenzene derivatives.[7] Experimental results show retarded appearance and full disappearance of a grating at characteristic times. The reason for the grating disappearance was not fully clarified. It was suggested that the diffraction grating recording mechanism is based on the growth of photoinduced isotropic phase domains.

In these studies, instead of uniform light intensity distribution, we used a laser with a Gaussian profile of the light intensity. Interference of two coherent laser beams leads to the sinusoidally modulated Gaussian distribution. Irradiation of such a material with periodically modulated light intensity leads to the formation of a phase-type diffraction grating, while periodic modulation of the refractive index in the dielectric material is formed.

In this article, we present results of in vivo microscopic observations of diffraction grating formation in a nematic azobenzene derivative, which let us propose a one-dimensional model describing the recording mechanism. The model is verified by fitting the results of serial experiments with different recording parameters.

2. EXPERIMENTAL SECTION

4-Heptyl-4′-methoxyazobenzene exhibiting a nematic phase close to room temperature (Cr 34.0 N 62.9 I) was used as a photochromic liquid crystal. Detailed description of the synthesis of this type of compound can be found in the article of J. Zienkiewicz et al.[10] For investigation of processes concerned with the studied materials, the sandwich-like sample, the so-called liquid-crystal panel (LCP), was prepared. Pure azobenzene derivative was heated up above the melting temperature and inserted between two glass plates. The sample used in the holographic recording experiment had a thickness of around 2 μm.

For the in vivo observation of dynamic diffraction grating formation by the Nd:YAG laser at $\lambda_r = 532$ nm, we used the polarized microscope with the heating stage, which allowed us to make the measurements in the nematic phase of the studied

Received: January 19, 2012
Revised: February 22, 2012
Published: February 23, 2012

   dx.doi.org/10.1021/jp3006662 | J. Phys. Chem. B 2012, 116, 3264−3269

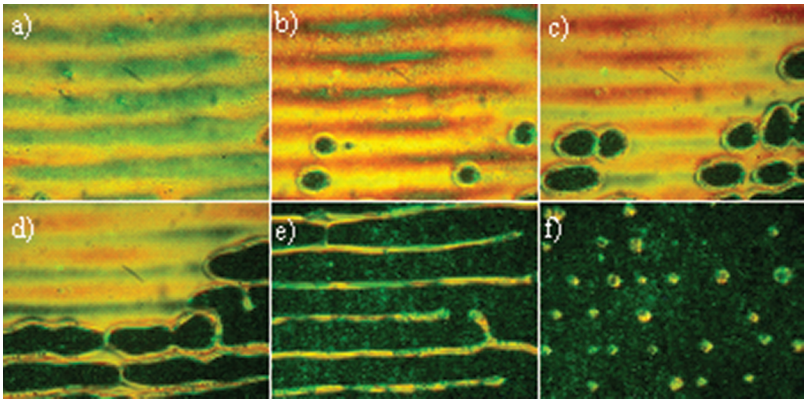

Figure 1. Micrographs of in vivo observations under the polarized microscope of diffraction grating recording and their temporal evolution for the steady illumination with characteristic interference pattern. The period of the grating Λ was about 50 μm.

material. Microscopic images were collected by an external camera. The period of the grating Λ was set to about 50 μm.

For the diffraction grating recording, two Gaussian profile beams of the Nd:YAG laser (Coherent Compass M315 100, λ_r = 532 nm) or the Ar^+ laser (Coherent Innova 90, λ_r = 514 nm) were used. Excitation at both wavelengths induced a trans−cis photochromic reaction. The total light intensity of each beam I_r was set to 41.7 mW/cm^2 (for λ_r = 532 nm) or 28.3 mW/cm^2 (for λ_r = 514 nm). The period of the grating was set also to about 50 μm. The sample was inserted into a heating system, and the temperature was set to 45 °C (apparatus error within ±3 °C). The light intensity of the first diffraction order during the grating recording was measured by a photodiode (Thorlabs PDA 55) and registered by an oscilloscope (Tektronix TDS 2024B). In the case of recording at 532 nm, an additional laser diode (λ = 633 nm) was used for the grating probing at a probing angle of $\beta \approx 5°$.

We have checked the influence of the (a) recording light intensity, (b) grating period, and (c) temperature on the grating recording dynamics. The recording conditions were as follows: $\beta \approx 5°$, λ_r = 532 nm, (a) Λ = 18 μm, T = 45 °C, 7.9 ≤ I_r ≤ 156 mW/cm^2, (b) I_r = 156 mW/cm^2, T = 45 °C, 1.37 ≤ Λ ≤ 18 μm, and (c) I_r = 70.8 mW/cm^2, Λ = 1.2 μm, 34 ≤ T ≤ 59 °C, respectively.

3. MICROSCOPIC OBSERVATION

As was mentioned above, the qualitative analysis of dynamic diffraction grating recording and molecular motions of studied compounds, according to the interference pattern created by laser light, was done with the use of a polarized microscope. In Figure 1, there are example micrographs that show temporal evolution of diffraction grating formation, based on the appearance of isotropic domains, which under the crossed polarizers are seen as a black color. The isotropic phase appears as domains after a certain recording time. Their appearance we explain as photoinduction of cis isomers of photochromic molecules, which disturbs the liquid-crystalline phase, causing the N → I phase transition.[1,9]

The nuclei of the isotropic phases appear at centers of bright fringes of the interference pattern, which can be seen in Figure 1b and c (black circle-shaped domains). The isotropic domains grow in regions of bright fringes, reaching the moment, after a certain time, at which only the stripes of the nematic phase are observed (cf. Figure 1e). Finally, the isotropic phase expands also into dark fringes of the interference pattern, vanishing the nematic phase, first by formation of liquid-crystalline droplets (cf. Figure 1f) and the then completely, causing the disappearance of the diffraction grating.

4. THEORETICAL APPROACH FOR THE GRATING FORMATION

Continuous light irradiation of photochromic compound leads to the creation of a critical cis isomer concentration (c^*_{cis}), causing the phase transition from the nematic to isotropic state.[9] The number of cis isomers created by light depends on such parameters like light intensity, absorption coefficient at a given wavelength, and quantum yield of trans−cis photoisomerization.

For the simplicity of the model, we assume that the temporal cis concentration up to the time of photoinduced phase transition is proportional to the irradiation time, while in azobenzene systems, this process generally occurs at low cis concentration. The time, during the sample irradiation, that is necessary for the creation of the local critical concentration of the cis isomer and phase transition is the so-called incubation time (t_0).

Nonuniform light intensity in the interference pattern (a sinusoidally modulated Gaussian shape was used in the experiment) has significant influence on the incubation time, which is distributed with respect to the position on the sample. Distribution of the incubation time along one direction in the plane of the sample $t_0(x)$ depends on the light intensity distribution $I(x)$ and is described by eq 1

$$t_0(x) = \frac{c^*_{cis}}{k \cdot I(x)} \tag{1}$$

where k is a constant comprised of the absorption coefficient and quantum yield and $I(x)$ is the light intensity distribution.

Two Gaussian beams are incident at the same region on the sample (with the center at x = 0), generating an interference pattern. Taking into account the one-dimensional cross section along the grating vector in the plane of the sample, the light intensity distribution is a sinusoidally modulated Gaussian function (Figure 2). The light intensity at the center of the mth interference maximum (at position $x = m \cdot \Lambda$) is expressed by a function dependent on the number of the interference maximum

$$I(m) = I_0 \cdot e^{-(m\Lambda/w)^2} \tag{2}$$

dx.doi.org/10.1021/jp3006662 | J. Phys. Chem. B 2012, 116, 3264−3269

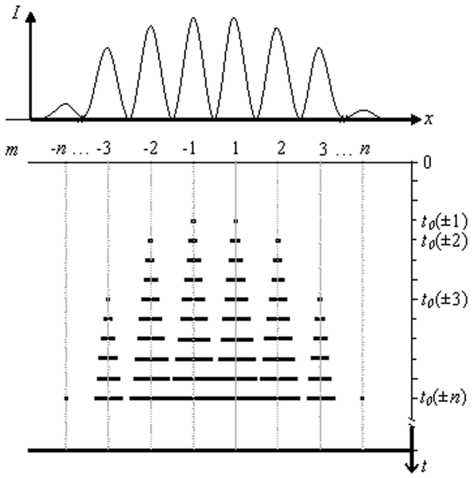

Figure 2. Sinusoidally modulated Gaussian light intensity distribution and schematic one-dimensional illustration of isotropic domains (black stripes) appearance in interference maxima and their growth during diffraction grating recording. The incubation time of a domain in the mth maximum $t_0(m)$ is presented on the time scale. $\pm n$ is the numbers of outermost interference maxima at a given time.

where m is the number of the interference maximum with respect to the center ($m = \pm1, \pm2, ..., \pm n$), $\pm n$ are the numbers of outermost interference maxima, $I_0 = I(0)$ is the maximum light intensity, and w is width of the Gaussian beams.

To determine the incubation time of the domain at the mth interference maximum $t_0(m)$, we described the position (x) as a function of m using the eq 1, and we used eq 2 to obtain the following formula

$$t_0(m) = \tau_0 \cdot e^{(m\Lambda/w)^2} \tag{3}$$

where $\tau_0 = (c^*_{cis})/(k \cdot I_0)$ is the minimal incubation time, related to the appearance of the domain at the central interference maximum.

Each isotropic domain appears at the interference maximum at a different time, which can be calculated from eq 3, and grows continuously. Figure 2 schematically shows the illustration of the one-dimensional model based on the appearance and growth of the isotropic domains.

For description of the domains size a_m we have assumed that each domain appears at a characteristic incubation time related to eq 3 and grows one-dimensionally from their centers until they reach the size of the grating period Λ (cf. Figure 2)

$$a_m = 2g[t - t_0(m)]^p \quad \text{for } t \geq t_0(m),\ a_m \leq \Lambda \tag{4}$$

where a_m is the width of the mth domain, g is the growth rate factor [m/s^p], and p is the growth time exponent.

We studied the growth of single domains, captured by video camera (cf. Figure 1), and have concluded that the growth of the domain's diameter can be represented by eq 4 with a time exponent p in the range of 0.3−0.45.

There were many studies about the kinetics of phase transition. Kolmogorow and Avrami in the late 1930s studied the kinetics of a thermally induced phase transition, assuming a linear growth rate of the domains ($p = 1$).[11] However, now, it is known that the growth rate can be not only linearly dependent on the function of time but described by an exponent equal to, for example, 1/3 or 1/2, which is a consequence of the mechanism of the phase change processes.[12,13] Moreover, two regimes during the dynamic domain growth characterized by different growth time exponents equal to 1.0 and about 0.4 have been reported in a previous article.[14]

Light diffracted on the sample gives information about its temporal structure. The light intensity distribution observed at a long distance behind a grating, composed of symmetrically distributed slits of various size, like, for example, those in Figure 2, can be expressed by the following relation

$$I(\theta) \propto \left[\sum_{m=1}^{n} a_m \frac{\sin\left(\frac{\pi \cdot a_m \sin\theta}{\lambda}\right)}{\frac{\pi \cdot a_m \sin\theta}{\lambda}} \cos\left(\left(m - \frac{1}{2}\right)\frac{2\pi}{\lambda}\Lambda \sin\theta\right) \right]^2 \tag{5}$$

where θ is the diffraction angle, a_m is the width of the mth slit, and λ is the probing wavelength.

In our simulations, an angle of the first diffraction order (θ_1) was calculated from the relation

$$\theta_1 = \arcsin\left(\frac{\lambda}{2\Lambda}\right) \tag{6}$$

The spread of the slits' size causes spatial broadening of first diffraction order; therefore, the light intensity in the first diffraction order I_1 was calculated as a sum of intensities for angles in a range of $\theta = \theta_1 \pm 0.1°$, which agrees with the detector readout range in the experimental setup. For the experimental data fitting, we used first-order diffraction intensity dynamics $I_1(t)$.

5. RESULTS AND DISCUSSION

At first, we compared recording at two different wavelengths. Figure 3 shows the temporal evolution of the first-order diffraction intensity for the grating period of $\Lambda = 50$ μm. We fitted the experimental data with the use of a proposed model (eq 6) using the time exponent of the growth process $p = 0.4$ (cf. eq 4), but the results were not satisfactory enough for the first curve. In order to find the appropriate time exponent p for the description of the domain growth process in this system, we used two different time exponents equal to 0.5 and 1 for fitting the above-mentioned data.

The shape of a curve assuming linear domain growth (growth time exponent $p = 1$) seems to be more similar to the experimental data at the start of the recording. On the other hand, the growth time exponent $p = 0.5$ gives better fitting results of the recording process, generally. Comparing the time exponent influence on the fitting results for further experiments, we concluded that time exponent $p = 0.5$ gives more accurate results than $p = 1$; therefore, we decided to perform fitting using the first. The difference in the fitting results can be related to the two regimes of the growth process or assumption of limited dimensionality of the studied system.

For verification of the proposed model, we experimentally checked the recording light intensity, grating period, and temperature influence on first-order diffraction intensity dynamics, and we fitted the experimental data using the proposed model. Selected experimental results together with theoretical fits are presented in Figure 4.

The presented model is based on three parameters, the growth time exponent p, growth rate factor g, and minimal incubation time τ_0, and can be used for fitting the experimental curves with good approximation. There are some differences in

dx.doi.org/10.1021/jp3006662 | J. Phys. Chem. B 2012, 116, 3264−3269

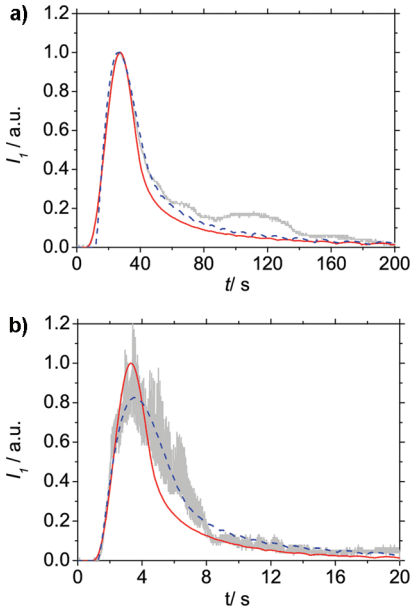

Figure 3. First-order diffraction intensity dynamics for recording a grating with a period of 50 μm at λ_r = (a) 532 and (b) 514 nm. Both graphs show experimental data (light gray line) and theoretical fits (for $a_m(t) \approx t^1$ (solid line) and $a_m(t) \approx t^{0.5}$ (dashed line)). Growth rate factors were as follows: (a) $g_{0.5} = 4.2\ \mu m \cdot s^{-0.5}$, $g_{1.0} = 0.7\ \mu m \cdot s^{-1}$ and (b) $g_{0.5} = 10.4\ \mu m \cdot s^{-0.5}$, $g_{1.0} = 6.4\ \mu m \cdot s^{-1}$, where $g_{0.5}$ and $g_{1.0}$ stand for the growth rate factors for fitting with p = 0.5 and 1.0, respectively. Recording parameters are mentioned in the Experimental Section.

the shape of the experimental and theoretical curves. The oscillations on the experimental curves (Figure 3 and 4) are related to the statistical nature of the phase transition. The remaining deviations can be related to the dimensionality of the studied system or probably the complex mechanism of the domains' growth, which is studied below. The growth rate factor dependence on recording parameters is used for this purpose.

The increase of the domain growth rate factor with the increase of the recording light intensity (Figure 5a) can be related to the faster cis isomer production by light. Thus, the phase transition is enforced in the whole interference region. On the other hand, the higher concentration gradient of the cis isomer molecules between the interference maximum and minimum speeds up the diffusion of these molecules, which will accelerate the growth process.

The fact that the rate of the growth process is concerned with the rate of the cis isomer production by light is also confirmed by the grating period influence. The growth rate factor (Figure 4b and Figure 5b) shows a generally increasing tendency with the grating period. The dependence can be explained in a way that the interference fringes (which have a bell shape) spread over a wider region in the case of the higher period of the interference pattern (cf. Figure 2). Such a difference causes the appearance of an isotropic phase in the same time but over a wider region, increasing the growth rate factor g.

On the other hand, each isotropic domain needs more time to cover the full distance of the grating period with an increase of its size, which is shown by extending the grating existence time (Figure 4b). It suggests that the growth is also related to the spontaneous movement of the molecules.

The growth rate factor dependence on temperature exhibits an Arrhenius-type relation (cf. Figure 5c)

$$g = g_0 e^{-E/RT} \tag{7}$$

where g_0 is the domain growth rate factor at infinite temperature, E is the activation energy of the growth process, and R is the gas constant.

Such a temperature dependence can confirm the influence of molecular diffusion on the growth of the domains, while the

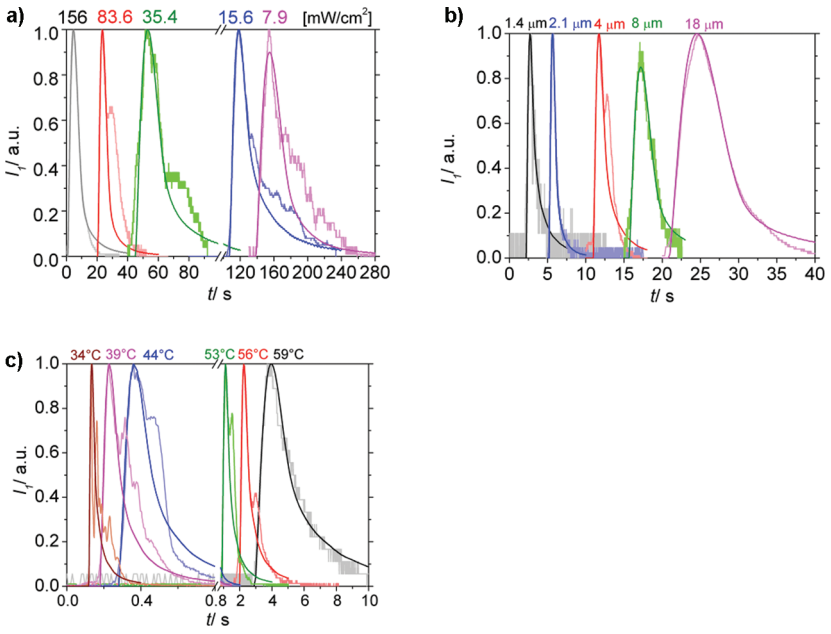

Figure 4. (a) Recording light intensity, (b) grating period, and (c) temperature influence on first-order diffraction intensity dynamics. Experimental data (light color) are fitted with a theoretical model (appropriate dark color) using eqs 4 and 5 and with the assumption p = 0.5. The curves in graph (a) are shifted consecutively in time by 0, 20, 40, 80, and 130 s; in (b), they are shifted by the multiplicity of 5 s. Experimental conditions are mentioned in the Experimental Section.

dx.doi.org/10.1021/jp3006662 | J. Phys. Chem. B 2012, 116, 3264−3269

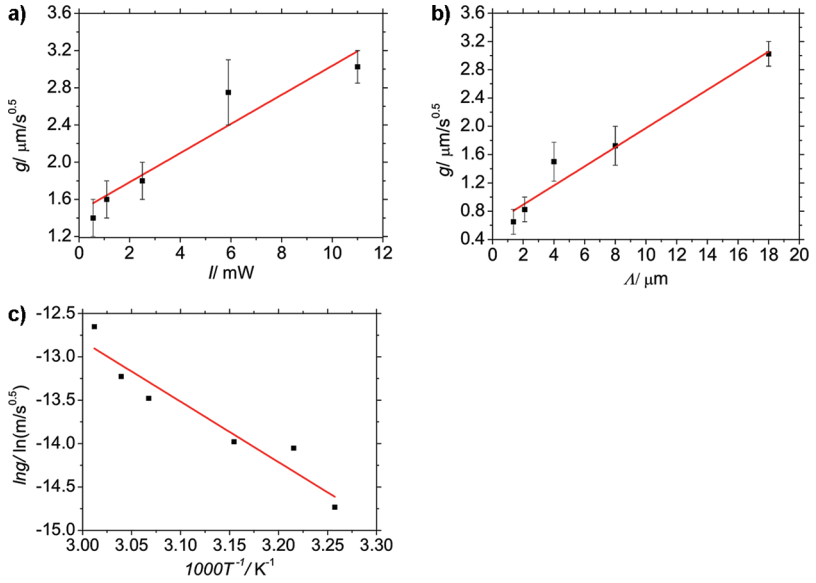

Figure 5. Linear dependence of the (a) recording light intensity and (b) grating period on the growth rate factor g and (c) Arrhenius-type relation between the growth rate factor and temperature, obtained by fitting the experimental data. The error was estimated as the standard deviation of the mean value, obtained by a few measurements. Experimental conditions are mentioned in the Experimental Section.

diffusion process is thermally activated. We have determined the activation energy for the growth process, which is equal to 57.9 kJ/mol, and the g_0 factor, equal to 3.23×10^9 μm·s$^{-0.5}$.

In this section, it was shown that by adjusting the recording parameters, such as the recording light intensity, grating period, and temperature, one can control the growth rate and temporal and maximal size of the isotropic domains during the grating recording process.

6. CONCLUSIONS

The mechanism of the grating recording in low molecular azobenzene derivative liquid crystals was proposed. Microscopic studies showed that diffraction grating formation is caused by the photoinduction of isotropic domains at interference maxima. The proposed model assumes a locally induced N → I phase transition by exceeding the critical cis isomer concentration.

The real situation in planar cell is illustrated by the one-dimensional model. The growth of isotropic domains in one dimension with growth time exponent $p = 0.5$ gives a good approximation to the experimental results. Deviations between the experimental and theoretical results are related to the statistical nature of the phase transition, limited dimensionality of the model, or complexity of the domains' growth mechanism.

The results obtained by fitting experimental curves indicate that the growth process of the domains can be complex and should assume two factors, stimulated production of cis isomer molecules in the neighborhood of the domain and spontaneous movement of these molecules. Both lead to the reaching of a local critical concentration, causing the phase transition.

The proposed model describes the processes occurring in the material during grating recording in the nematic azobenzene derivative. It can be easily modified; for example, one can change the appearance time distribution of the domains by changing the beam intensity profile. Concluding, this can be helpful for the prediction and simulation of the temporal domains' size distribution during the grating recording process. The control of the domains' size can be useful for the dynamic photonic devices, based on gratings or domains of size at the microscopic level. However, some further attention should be paid to the origins of the growth.

AUTHOR INFORMATION

Corresponding Author

*E-mail: maciej.czajkowski@pwr.wroc.pl. Phone: +48 713202317. Fax: +48 713203364.

Notes

The authors declare no competing financial interest.

ACKNOWLEDGMENTS

The authors thank Z. Galewski (University of Wroclaw) for providing the material for the research. The work was financially supported by Grant No. NN 507 475237 statutory activity subsidy from the Polish Ministry of Science and Higher Education for the Faculty of Chemistry of Wroclaw University of Technology and Grant No. 2011/01/B/ST8/03317 from the Polish National Science Centre.

REFERENCES

(1) Ikeda, T.; Tsutsumi, O. *Science* **1995**, *268*, 1873−1875.
(2) Tong, X.; Zhao, Y. *Chem. Mater.* **2009**, *21*, 4047−4054.
(3) Lansac, Y.; Glaser, M. A.; Clark, N. A.; Lavrentovich, O. *Nature* **1999**, *398*, 54−57.
(4) Ikeda, T.; Tsutsumi, O.; Sasaki, T. *Synth. Met.* **1996**, *81*, 289−296.
(5) Hrozhyk, U. A.; Serak, S. V.; Tabiryan, N. V.; Hoke, L.; Steeves, D. M.; Kimball, B. R. *Opt. Exp.* **2010**, *18*, 8697−8704.
(6) Matczyszyn, K.; Bartkiewicz, S.; Sahraoui, B. *Opt. Mater.* **2002**, *20*, 57−61.
(7) Czajkowski, M.; Mysliwiec, J.; Zygadlo, K.; Galewski, Z.; Bartkiewicz, S. *Chem. Phys. Lett.* **2011**, *510*, 131−134.
(8) Sung, J.-H.; Hirano, S.; Tsutsumi, O.; Kanazawa, A.; Shiono, T.; Ikeda, T. *Chem. Mater.* **2002**, *14*, 385−391.
(9) Matczyszyn, K.; Sworakowski, J. *J. Phys. Chem. B* **2003**, *107*, 6039−6045.
(10) Zienkiewicz, J.; Galewski, Z. *Pol. J. Chem.* **2002**, *76*, 359−366.
(11) Avrami, M. *J. Chem. Phys.* **1939**, *7*, 1103−1112.

(12) Bronnikov, S.; Dierking, I. *Phys. Chem. Chem. Phys.* **2004**, *6*, 1745−1749.
(13) Diekmann, K.; Schumacher, M.; Stegemeyer, H. *Liq. Cryst.* **1998**, *25*, 349−355.
(14) Bronnikov, S.; Nasonov, A.; Racleş, C.; Cozan, V. *Soft Mater.* **2008**, *6*, 119−128.